Stable Forearc Stressed by a Weak Megathrust: Mechanical and Geodynamic Implications of Stress Changes Caused by the M = 9 Tohoku‐Oki Earthquake

doi: 10.1029/2018JB017043

JGR Solid Earth

RESEARCH ARTICLE
10.1029/2018JB017043

Special Section:
Stress at Active Plate Boundaries - Measurement and Analysis, and Implications for Seismic Hazard

Stable Forearc Stressed by a Weak Megathrust: Mechanical and Geodynamic Implications of Stress Changes Caused by the M = 9 Tohoku-Oki Earthquake

Kelin Wang[1], Lonn Brown[2], Yan Hu[3], Keisuke Yoshida[4], Jiangheng He[1], and Tianhaozhe Sun[5]

[1]Pacific Geoscience Centre, Geological Survey of Canada, Sidney, British Columbia, Canada, [2]International Seismological Centre, Thatcham, UK, [3]Mengcheng National Geophysical Observatory, School of Earth and Space Sciences, University of Science and Technology of China, Hefei, China, [4]Research Center for Prediction of Earthquakes and Volcanic Eruptions, Graduate School of Science, Tohoku University, Sendai, Japan, [5]Department of Geosciences, Pennsylvania State University, University Park, PA, USA

Key Points:
- Stress reversal in offshore forearc due to the Tohoku-Oki earthquake indicates weak subduction megathrust with effective friction ~0.032
- Most of the forearc is under very low differential stress and is stable throughout subduction earthquake cycles except the outer wedge
- Earthquakes and active faulting in a strong and stable forearc reflect heterogeneities in structure, stress, and/or pore fluid pressure

Supporting Information:
- Supporting Information S1
- Data Set S1
- Data Set S2
- Data Set S3

Correspondence to:
K. Wang,
kelin.wang@canada.ca

Citation:
Wang, K., Brown, L., Hu, Y., Yoshida, K., He, J., & Sun, T. (2019). Stable forearc stressed by a weak megathrust: Mechanical and geodynamic implications of stress changes caused by the M = 9 Tohoku-Oki earthquake. *Journal of Geophysical Research: Solid Earth*, *124*, 6179–6194. https://doi.org/10.1029/2018JB017043

Received 16 NOV 2018
Accepted 23 MAY 2019
Accepted article online 31 MAY 2019
Published online 29 JUN 2019

Abstract Rupture-zone averaged static stress drop in the 2011 M=9 Tohoku-Oki earthquake was less than 5 MPa, but it caused a stress reversal in most of the offshore forearc, although the reversal is less well constrained far offshore by earthquake mechanisms because of 20- to 30-km errors in event depths. Using a finite element model of force balance, we demonstrate that the stress reversal unambiguously indicates (1) a very weak subduction megathrust and (2) very low differential stresses in the forearc. Prior to the reversal, the upper limit of megathrust strength could not be determined from forearc stresses. In the forearc, effects of megathrust friction and gravity are in a fragile balance, and stresses fluctuate around a neutral state in earthquake cycles. If most of the offshore forearc is to be compressive before but extensional after the earthquake, the effective friction coefficient of the megathrust must be ~0.032. Under low differential stresses associated with megathrust weakness, the forearc is generally well below yielding. Applying the concepts of dynamic Coulomb wedge, we show that the inner wedge, and by inference farther landward, stays stable throughout earthquake cycles. The outer wedge is stable most of the time but may occasionally enter a critical state during great earthquakes; its geometry suggests that complete stress drop of the underlying shallow megathrust is unlikely to have happened. We reason that the occurrence of earthquakes and active faulting under low stress in the stable forearc is due to heterogeneities in structure, stress, and/or pore fluid pressure.

1. Introduction

The type of force-balance model illustrated in Figure 1a is widely used to study forearc stresses and megathrust strength. The principle of the model is similar to that of a critically tapered or stable Coulomb wedge (Dahlen, 1984; Wang & Hu, 2006) in which megathrust strength is represented by an effective coefficient of friction μ_b', the ratio of the shear and normal stresses on the fault (Figure 1c). In the presence of margin topography, the tendency for gravitational collapse induces (deviatoric) margin-normal horizontal tension in the forearc, but the shear stress along the megathrust tends to generate margin-normal compression. To first order, the state of stress in the cross-sectional view of Figure 1a is the consequence of this "competition."

Despite differences in model assumptions and simplifications, the application of the force-balance model by different authors has consistently led to the inference of weak subduction megathrusts. Values of μ_b' determined by Wang and He (1999), Wada and Wang (2005), Lamb (2006), and Seno (2009) are within the range of 0.01–0.1, much lower than the value of around 0.4 based on Byerlee's law (Byerlee, 1978) assuming hydrostatic pore fluid pressure. Some models that are based on the same force-balance concept but assume a viscous lithosphere, designed for long-term deformation such as mountain building, invoked similarly weak megathrusts (Luo & Liu, 2009; Sobolev & Babeyko, 2005). By using heat flow observations to constrain frictional heating along the megathrust for a number of subduction zones, Gao and Wang (2014) found that a μ_b' value around 0.03 is common, although values greater than 0.1 are also seen depending on the roughness of the subducting seafloor. While the previous studies address the fault and/or forearc stresses in the long term or at a given time, the present paper addresses temporal stress changes. Our focus is

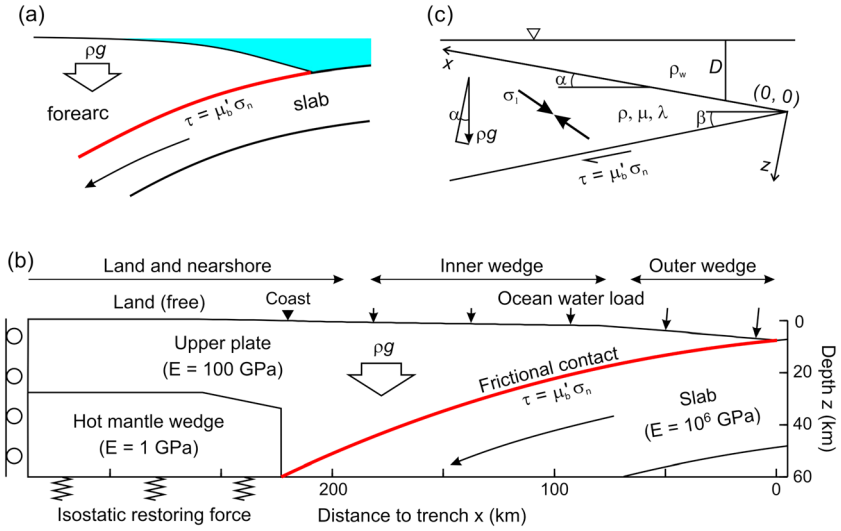

Figure 1. Conceptual and mathematical models discussed in this work. (a) Main forces controlling forearc stress. Here ρ is rock density, g is gravitational acceleration, μ_b' is effective coefficient of friction, and τ and σ_n are, respectively, shear and normal stresses on the fault. (b) Structure and boundary conditions of the elastic stress model discussed in section 3. E is Young's modulus. (c) The Coulomb wedge model to be discussed in section 4, showing the coordinate system (x, z), example maximum compressive stress σ_1, surface slope angle α, basal dip β, and water depth D. Here ρ_w is water density, μ is coefficient of internal friction, and λ is pore fluid pressure ratio defined in equation (1).

primarily on the offshore forearc, which, in the terminology of the dynamic Coulomb wedge theory (Figure 1c; Wang & Hu, 2006), consists of the inner wedge and outer wedge (Figure 1b). By analyzing stress changes in the forearc caused by the 2011 magnitude (M) 9 Tohoku-Oki earthquake, we study the following two outstanding issues.

The first outstanding issue is the upper limit of megathrust strength. Prior to the Tohoku-Oki earthquake, earthquake focal mechanisms consistently indicated predominantly margin-normal compression ($\sigma_x > \sigma_z$) throughout the forearc, arc, and backarc at the Japan Trench margin. Without knowing by how much σ_x was larger than σ_z, the strength of the megathrust could not be determined using the aforementioned force balance argument. Wang and Suyehiro (1999) hypothesized that a μ_b' value as low as 0.03 was possible for the Japan Trench, but they showed that very high values could also be consistent with forearc stress observations. Lamb (2006) inferred $\mu_b' \approx 0.032$ by assuming $\sigma_x - \sigma_z = 0$ around the volcanic arc without using stress observations. Seno (2009) inferred $\mu_b' = 0.017$ by applying a value of $\sigma_x - \sigma_z = 50$ MPa based on estimates of tectonic forces that may contain very large errors. Based on stress orientations inferred from the aftershocks of a 1968 M = 8.2 megathrust earthquake north of the 2011 rupture, Magee and Zoback (1993) proposed a very weak megathrust, but only for a limited area. In the present study, we will show that the stress change in the forearc caused by the 2011 Tohoku-Oki earthquake allows us to determine the upper limit of the megathrust strength.

The second outstanding issue is the mechanical strength and stability of the forearc, particularly the wedge-shaped offshore part (Figure 1b). Is the forearc crust critically stressed, that is, everywhere on the verge of failure? How weak or strong is the forearc crust as compared to the megathrust? There is speculation that the forearc crust is as weak as the megathrust (e.g., Bürgmann, 2015; Hardebeck, 2015). If so, would we still expect plate convergence to be accommodated by the megathrust, with the forearc being generally of low topographic relief and structurally stable over geological time scales? On the other hand, if the crust is strong and stable, why do we still observe seismicity and active faulting in it? What can we infer about megathrust stress drop in great earthquakes from the stability state and geometry of the inner and outer wedges? Could the outer wedge become so unstable during the 2011 earthquake that a major normal fault slipped by many meters (McKenzie & Jackson, 2012)? In this study, we apply the theory of dynamic Coulomb wedge (Wang & Hu, 2006) and discuss what the forearc stress change due to the Tohoku-Oki earthquake tells us about the mechanical state of the forearc in subduction earthquake cycles.

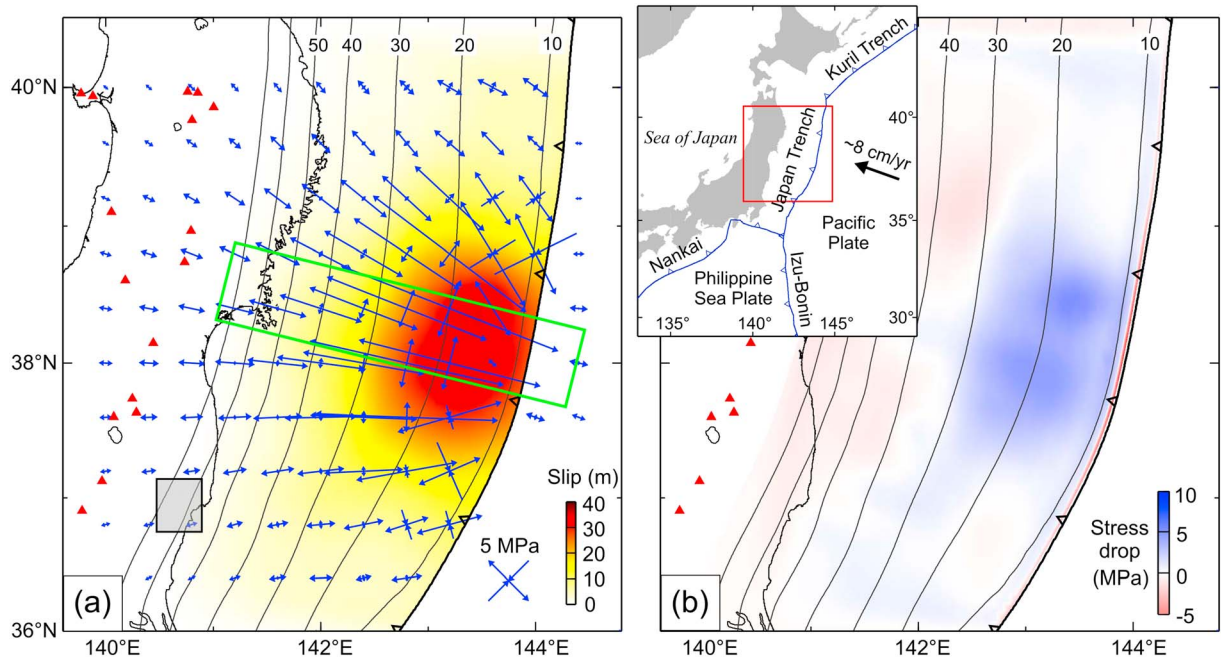

Figure 2. Model predicted coseismic stress changes in the 2011 Tohoku-Oki earthquake. Red triangles mark locations of active volcanoes. Depth of the plate interface is contoured in kilometer (labeled curves). Inset shows regional tectonics around the map area (red box). (a) Principal stresses at the model upper surface. Stresses at 10–20 km are similar except near the trench. Divergent arrow pairs indicate incremental tension. The coseismic slip distribution along the megathrust used in this model is an average of 43 published models (Sun et al., 2017). Details of the finite element model and comparison with geodetic observations are provided by Wang et al. (2018). Green box approximately indicates the corridor of seismicity shown in Figure 3. The gray rectangle approximately marks the location of the small area of anomalous stress discussed at the end of sections 2.1 and 4.4. (b) Stress drop along the megathrust calculated from the average slip model using the method described in Brown et al. (2015).

2. Stress Change in the Forearc Caused by the Earthquake

2.1. Stress Change Based on Earthquake Focal Mechanisms

Many models of coseismic slip distribution have been constructed for the Tohoku-Oki earthquake by inverting different types of observations including seismological (e.g., Ide et al., 2011; Shao et al., 2012), geodetic (e.g., Iinuma et al., 2012), and tsunami (e.g., Satake et al., 2013) data. Figure 2a shows the average slip distribution of 43 published models, which fits coseismic geodetic observations very well in a three-dimensional (3-D) finite element model (Wang et al., 2018). Figure 2a also shows perturbations to crustal stresses predicted using this 3-D model.

All the published slip models yield a fault stress drop less then 5 MPa if averaged over the area encompassed by the 5-m slip contour (Brown et al., 2015). The stress drop distribution derived from the average slip model is shown in Figure 2b. It is remarkable that such a seemingly small stress drop changed the state of stress in the offshore forearc from predominantly margin-normal compression to tension. The stress reversal was documented by a number of studies through analyses of focal mechanisms of small earthquakes off the megathrust before and after the earthquake (Asano et al., 2011; Hasegawa et al., 2012; Nakamura et al., 2016; Okada et al., 2011; Yoshida et al., 2012). Results from Hasegawa et al. (2012) and Nakamura et al. (2016) along a central corridor (Figure 2a) are shown in Figure 3.

The focal mechanisms from Hasegawa et al. (2012; Figure 3a) are centroid moment tensor (CMT) solutions derived from broadband data recorded by the dense F-net and Hi-net seismic networks using the method of Ito et al. (2006). Nakamura et al. (2016) inherited CMT solutions from 1997 to 2013 in the F-net catalog and did not derive more CMT solutions. However, taking advantage of the similarity of waveforms between events of similar focal mechanisms recorded by the same seismic stations, Nakamura et al. (2016) were able to identify many more events that belong to different focal mechanism groups (Figure 3b) and expanded the event-type catalog back to 1984. Compared to the work of Hasegawa et al. (2012), Nakamura et al. (2016) reported over four times as many events that are classified into focal mechanisms groups, but the

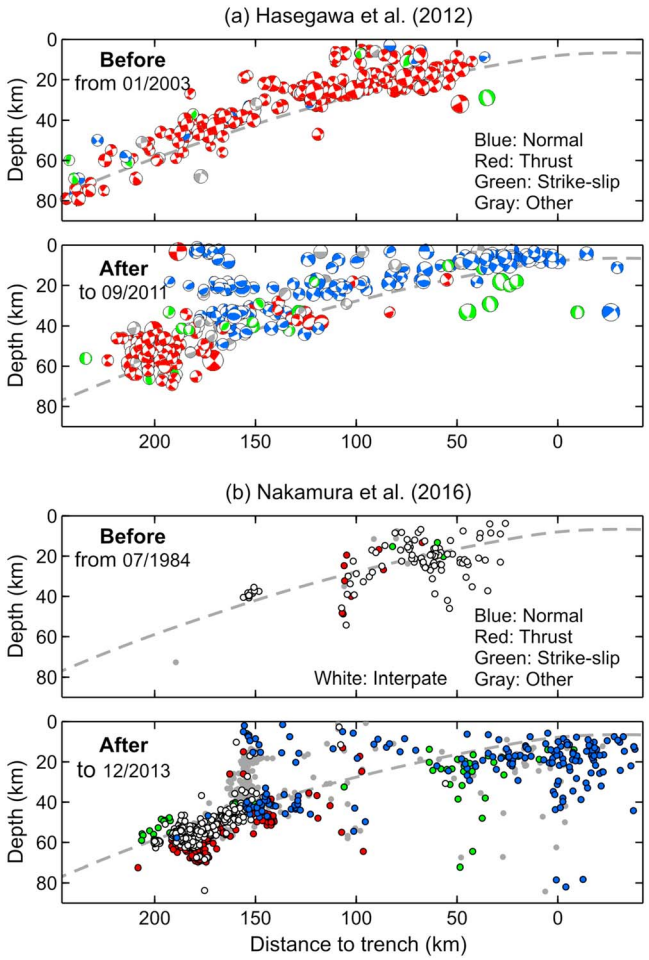

Figure 3. Focal mechanisms of earthquakes before and after the Tohoku-Oki earthquake approximately along the corridor shown in Figure 2a. Dashed line is the plate interface, a compromise of what was shown in the two referenced papers. (a) Mechanisms reported by Hasegawa et al. (2012) in side-view stereo net projection ("beach balls"). Thrust events include both interplate events and those off the fault. (b) Mechanisms reported by Nakamura et al. (2016) in color coded categories. Nakamura et al. (2016) separated thrust events into interplate events (white) and noninterplate thrust events (red) according to their Kagan's angles.

accuracy of individual solutions is generally lower. Along a similar corridor (Figure 2a), Nakamura et al. (2016) reported fewer upper-plate thrust events before the Tohoku-Oki earthquake than did Hasegawa et al. (2012; Figure 3). This difference to some degree reflects the difficulty in deciding which subset of thrust events is on the megathrust (interplate events). After the earthquake, the prevalence of upper-plate normal-faulting events reported by Nakamura et al. (2016) is consistent with Hasegawa et al. (2012; Figure 3).

The central corridor shown in Figure 3 is representative of the first-order state of stress in a broader segment of the offshore forearc and its change caused by the Tohoku-Oki earthquake (Hasegawa et al., 2012). In detailed map view, the stress field before the earthquake exhibited much heterogeneity at both regional and local scales (Yoshida et al., 2015a, 2016). The most notable departure from the general pattern of Figure 3 is in a near-coast area around 37° latitude (Figure 2a). In this small area, crustal earthquakes shallower than ~12 km are predominantly of the normal-faulting type both before (Imanishi et al., 2012; Yoshida et al., 2015a) and after (Kato et al., 2011; Okada et al., 2011; Yoshida et al., 2015b) the Tohoku-Oki earthquake, but the deeper ones are persistently of the reverse-faulting type (Yoshida, 2014). This local stress variation with depth is reminiscent of plate bending (Yoshida et al., 2015a), but the actual cause is not yet understood.

2.2. Errors in Earthquake Depths and Confidence in the Stress Reversal

If interplate events are not excluded, they seriously contaminate the inference of stresses in the upper plate. Identification of interplate events is thus a critical step of forearc stress analysis. Because the seismic networks are on land, depths of offshore events in network catalogs contain very large errors, such that the identification of interplate events cannot be based on the reported centroid or focal depths. The farther offshore, the more challenging is the depth determination. For this reason, we refrain from incorporating the results of stress analyses that used catalog event depths to distinguish between interplate and noninterplate events such as those in Hardebeck (2012, 2015).

Hasegawa et al. (2012) and Nakamura et al. (2016) did not rely on catalog depths. Instead, they followed the procedure of Asano et al. (2011) to identify interplate events based on focal mechanisms. Specifically, an event is considered interplate if its focal mechanism is within a defined range from that of a "theoretical" interplate thrust event based on the plate motion direction and megathrust geometry, measured using the Kagan's angle (Kagan, 1991). According to Nakamura et al. (2016), the vast majority of small earthquakes before the Tohoku-Oki earthquake along the central corridor were interplate events. The vertical scatter of the interplate events shown in Figure 3b, greater than 30 km on each side of the fault, reflects the large errors in their depth determination. Hasegawa et al. (2012) obtained more accurate depths by deriving CMT solutions, but they still assumed an error of up to ±20 km in their centroid depths.

Given the large uncertainties in event depths offshore, we do not base our analysis on the details of the stress inversion results such as those of Hasegawa et al. (2012). We only focus on the overall stress contrast before and after the Tohoku-Oki earthquake, which is adequately demonstrated by the earthquake focal mechanisms shown in Figure 3. Because the reliability of event depths deteriorates farther offshore, we place greater confidence in the events nearshore and in the inner wedge. There were relatively few focal mechanisms nearshore and in the inner wedge prior to the Tohoku-Oki earthquake, but these limited data including those outside of the central corridor (Hasegawa et al., 2012) do indicate compression in general. In

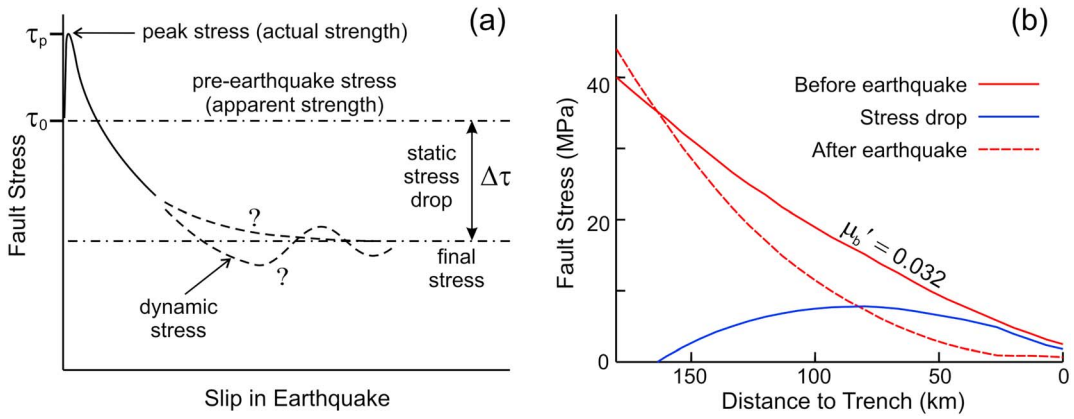

Figure 4. Shear stress and stress drop along the plate interface. (a) Schematic illustration of shear stress change at a point on the interface during a large earthquake. (b) Fault stress distribution assumed for the model shown in Figure 5. The before-earthquake distribution (apparent strength) is used for Figure 5a, "stress drop" for Figure 5b, and their difference "after earthquake" (final stress) for Figure 5c.

section 3.3, we will explain that compression nearshore and in most of the inner wedge before the earthquake is also theoretically expected. Therefore, there is good reason to believe that the Tohoku-Oki earthquake caused a stress reversal in these areas.

The situation of the outer wedge is not as clear as commonly perceived. Despite the great caution used by Hasegawa et al. (2012) and Nakamura et al. (2016) in identifying interplate events, there is still a possibility that some of the normal-faulting events shown in the outer wedge in Figure 3 actually belong to the subducting slab. With two months of close-range monitoring using a dense ocean bottom seismic network that started 5 months after the earthquake, Obana et al. (2013) detected some normal-faulting events only around the landward end of the outer wedge, a couple of reverse-faulting events about 20 km seaward, and no events in the wedge within 45 km of the trench. The normal-faulting events are consistent with the outer wedge being extensional, but it is not clear whether the few reverse-faulting events indicate that this part of the outer wedge never underwent stress reversal or regained compression within 5 months after the Tohoku-Oki earthquake. The presence of seafloor open fissures in the outer wedge area after the earthquake (e.g., Tsuji et al., 2013) may be direct evidence for the stress reversal, but there is uncertainty in whether these surficial fissures only represent slumping-like near-surface processes due to seismic shaking. Seemingly fresh seafloor scarps may indicate the activation by this earthquake of large normal faults seen in seismic images (Tsuji et al., 2011, 2013). Borehole breakout analyses in the tip of the outer wedge are consistent with a stress change from compressive to extensional due to the Tohoku-Oki earthquake (Brodsky et al., 2017; Lin et al., 2013). Therefore, even with the paucity of reliable focal mechanisms, we may still assume that stress reversal also occurred in the outer wedge.

3. Constraining the Strength of the Megathrust

3.1. Static Stress Drop in the Tohoku-Oki Earthquake

The effective coefficient of friction $\mu_b^{'}$ mentioned in section 1 is a composite parameter that includes the effects of both the intrinsic friction and pore fluid pressure in the fault zone, a point we will briefly revisit at the end of section 4.1. For megathrust faults that exhibit stick-slip behavior and produce great earthquakes, it represents the apparent strength, that is, the level of shear stress that the fault can sustain before a great earthquake (Figure 4a). The net decrease in this shear stress during the earthquake is the static stress drop (Figure 4a). Based on the "average model" in Figure 2b, we design a 2-D stress drop distribution (Figure 4b), to be used for the model described in the ensuing sections. The actual stress drop distribution must be very heterogeneous (Brown et al., 2015), but it is the long-wavelength (smoothed) stress drop that is of first-order importance to our analysis. Locally large values of stress drop or stress increase affect details of the forearc stress change, particularly in the outer wedge, but we have neither reliable local stress drop values nor reliable outer wedge stress indicators to address these details.

Stress perturbation in the forearc caused by the earthquake is certainly 3-D, but for the central corridor of a smooth version of the slip distribution (Figure 2a), a 2-D representation is reasonable. The thickness H of the offshore forearc is much smaller than the strike length of the rupture zone. Stress perturbations above the rupture zone along the central corridor are caused mainly by fault slip within ~2H of the corridor. At distances farther away, such as >50 km west of the coast, stress perturbation along the central corridor is slightly overestimated using our 2-D representation.

3.2. Force-Balance Model for Forearc Stresses

As explained in section 1, the state of stress in the onshore forearc before the Tohoku-Oki earthquake could not adequately constrain the apparent strength of the Japan Trench megathrust because we did not know by how much σ_x was greater than σ_z. Here we revisit this problem by considering stress observations not only before but also after the earthquake.

The force balance model we employ (Figure 1b) is almost a reproduction of the Japan Trench model of Wang and Suyehiro (1999). This plane-strain finite element model features two elastic plates in frictional contact. Gravitational acceleration is 9.8 m/s^2, and density is assumed to be uniformly 2,800 kg/m^3. Instead of assigning prestress, which is very difficult to handle for a model with real long-wavelength margin topography (Figure 1b), we use a Poisson's ratio of ~0.5 (incompressible), such that the modeled differential stress is due purely to the balance of fault friction and gravitational force like in a Coulomb wedge model (section 4; Wang & He, 1999). The subducting plate is assigned to be nearly rigid (Figure 1b). Its role is simply generating frictional shear stress along the plate interface.

The interface geometry is assigned a constant curvature to avoid spurious stresses due to fault motion against geometrical incompatibility, but otherwise, it is as close as possible to the observed megathrust geometry as shown in Figure 2. The problem of frictional contact is numerically handled using the method of domain decomposition with Lagrange multipliers and is detailed in Wang and He (1999). Downdip of the frictionally coupled area, the fault zone rheology transitions to thermally activated viscous creep at around 50- to 60-km depth, with the viscous stress depending on the strain rate of the creep zone (Gao & Wang, 2014). With the frictional seismogenic zone locked, the strain rate in the creep zone diminishes in the later part of the interseismic period. Therefore, for modeling stresses before the Tohoku-Oki earthquake the viscous stress is assumed to be negligibly small and ignored. During the earthquake, the deeper megathrust exhibits velocity strengthening or viscous strengthening, which is why the coseismic stress drop is limited to shallow depths (Figures 2b and 4b).

The load by ocean water offshore is modeled using a traction boundary condition (Figure 1b), with pressure values determined from water density and depth. With the dislocation creep rheology and very high temperature, there is little stress in the hot mantle wedge (Wada & Wang, 2009), except in the postseismic period when the strain rate can be high. Therefore, for modeling pre-earthquake stresses, the hot mantle wedge is regarded as an inviscid fluid, modeled using an extremely compliant but incompressible elastic material supported from below by a Winkler restoring force (Figure 1b; Wang & He, 1999; Wang & Suyehiro, 1999). The left boundary is 420 km from the trench, farther than shown in Figure 1b. One small difference from the model of Wang and Suyehiro (1999) is that the dividing boundary (at 250 km; Figure 1b) between the hot and the “cold nose” parts of the mantle wedge is more vertical, better reflecting the abruptness of the change in the thermal state and hence mechanical properties between these two regimes (Wada & Wang, 2009). The other difference is a denser finite element mesh with numerically better element geometry. These changes have made little difference to model results. Further details about the model can be found in Brown (2015).

3.3. Forearc Stresses Before and After the Earthquake

The preferred model before the earthquake is shown in Figure 5a in terms of 2-D deviatoric stresses; that is, the mean stress $(\sigma_x+\sigma_z)/2$ has been subtracted. The megathrust μ_b' value for this model is 0.032, the same as preferred by Wang and Suyehiro (1999) and Lamb (2006), and the shear stress distribution along the megathrust is shown in Figure 4b. This μ_b' value compares very well with that inferred by Gao and Wang (2014) based on frictional heating analysis. The slightly lower value (0.025) preferred by Gao and Wang (2014) is expected because frictional heat is generated mainly during seismic slip when the fault is dynamically weakened (Figure 4a).

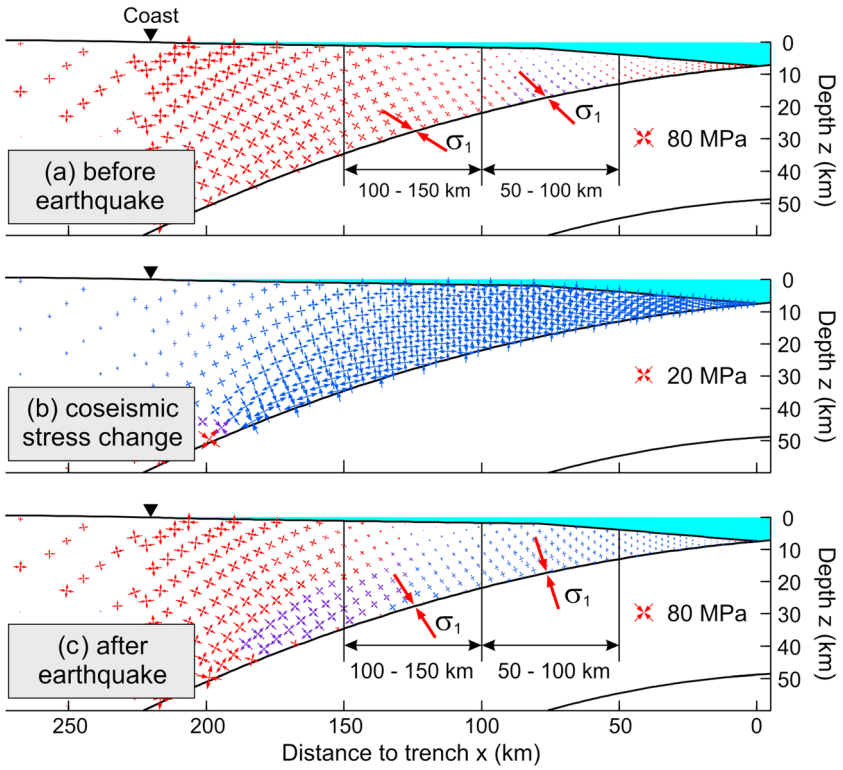

Figure 5. Preferred model of forearc stress change due to the Tohoku-Oki earthquake. Shear stress distributions along the megathrust for this model are shown in Figure 4. For stress crosses, red or blue indicates that the plunge of σ_1 is less than 40° (compression) or greater than 50° (tension), respectively, and purple indicates plunge between 40° and 50°. (a) Deviatoric stress before the earthquake. (b) Incremental change in deviatoric stress caused by the earthquake. (c) Deviatoric stress after the earthquake. The two segments for which average stress is evaluated (e.g., Figure 6) are marked in (a) and (c) with the orientation of near-fault σ_1 indicated.

Model tests (Brown, 2015) verify that there is greater deviatoric compression nearshore and in the landward part of the inner wedge than onshore for any μ_b' value. The lesser compression onshore is due to the higher elevation of the land area and thus greater gravitational effect. This theoretical expectation supports the notion of a slightly compressive inner wedge prior to the Tohoku-Oki earthquake discussed in section 2.2 above. Because the onshore area was observed to be compressive prior to the earthquake (except for shallow depths in the small area mentioned in section 2.1 and shown in Figure 2a), at least the landward part of the inner wedge is also expected to have been compressive.

To model the stress perturbation caused by the Tohoku-Oki earthquake, we use the stress drop distribution illustrated in Figure 4b. We do not model the time-dependent evolution of fault stress but only the net stress drop. The "before-earthquake" results (Figure 5a) are used as the starting condition, and rupture occurs in response to the imposed stress drop, releasing elastic strain energy and, by slightly changing surface elevation, gravitational energy. This is very different from the model of McKenzie and Jackson (2012) that was designed to illustrate only the effect of the gravitational energy. Deviatoric stresses in the forearc induced by this net stress drop are shown in Figure 5b. The level of stress perturbation and its landward decrease in this model are consistent with what is predicted by 3-D slip models (Figure 2a).

Deviatoric values of the resultant stress field after the earthquake are shown in Figure 5c. In this model, most of the offshore forearc is changed from compression to tension by the great earthquake. The plunge of the maximum compressive stress σ_1 becomes steeper as a result of this stress change. As will be discussed in section 4.3, the upper plate is generally below yielding in real Earth, and the use of an elastic model yields very reasonable results. However, near the surface in some areas, such as near the coast, model-predicted differential stresses are unreasonably large (Figures 5a and 5c). Introducing Coulomb-plasticity would alleviate the artifacts and would also slightly reduce differential stresses

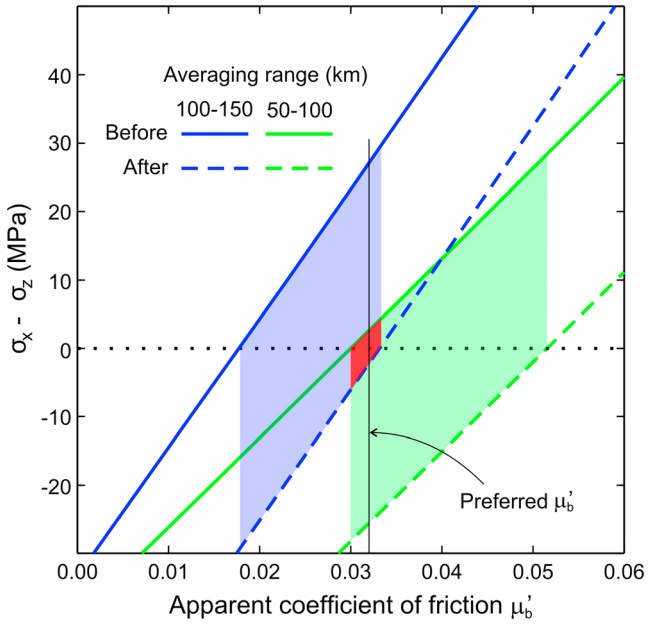

Figure 6. Spatial averages of $\sigma_x - \sigma_z$ for the two segments shown in Figure 5 for different values of megathrust μ_b'. The purple- or green-filled area shows the range of μ_b' in which the average $\sigma_x - \sigma_z$ in the 100- to 150-km or 50- to 100-km segment, respectively, meets the requirement of being compressive before the earthquake and extensional after the earthquake. The red area is the range in which both segments meet this requirement.

landward of the coast, but the improvement would be very small, especially for the offshore area. Obviously, throughout the interseismic period, fault stress will gradually recover from the postearthquake value (Figure 4b, dashed red line) to the pre-earthquake value (Figure 4b, solid red line), causing the forearc stress to change back to the state shown in Figure 5a. Fault stress can be constrained by forearc stress observations at any stage of this evolution, but only at the latest stage of the interseismic period when the fault is on the verge of seismic failure does the fault stress represent the apparent strength of the fault.

Our 2-D model does not fully describe the real subduction zone. For example, coseismic deformation caused very small incremental margin-parallel tension (Figure 2a), but it triggered normal-faulting earthquakes in the most landward part of the inner wedge reflecting margin-parallel extension (Figure 3a), which may indicate either a local prestress condition or local strength anisotropy. Nonetheless, for constraining megathrust strength using forearc stress, the comparison of σ_x with σ_z is the most relevant (Wang & He, 1999).

To explain why the model shown in Figures 4b and 5 is preferred, let us examine $\sigma_x - \sigma_z$ volumetrically averaged over each of the two segments marked in Figure 5 (50–100 km and 100–150 km). If the average $\sigma_x - \sigma_z$ is positive, the segment is mainly under horizontal compression, and vice versa. We construct models similar to that shown in Figure 5 for a range of megathrust μ_b' values (Figure 6). If in both segments the average stress is to be compressive before the earthquake but extensional after, the μ_b' value has to be in the range 0.030–0.0335 (Figure 6, red shaded area). Obviously, uncertainties in the magnitude of the long-wavelength stress drop affect the results. If the magnitude is lower than shown in Figure 4b, a lower value of μ_b' value will be required, and the pre-earthquake forearc will be less compressive than in Figure 5a. If the magnitude is higher than shown in Figure 4b, a higher value of μ_b' may be inferred, or the postearthquake forearc will be more extensional than shown in Figure 5c.

3.4. Fragility of the State of Stress in Offshore Forearc

The results described above deliver two important messages: (1) The megathrust must be very weak as earlier hypothesized by Magee and Zoback (1993), Wang and Suyehiro (1999), Lamb (2006), and Seno (2009) and similar to many other subduction zones, and consequently, (2) the forearc must be near the neutral state of stress $\sigma_x = \sigma_z$; that is, the differential stress must be rather small.

If, and only if, the differential stress is very small, the state of stress responds sensitively to seemingly benign spatial or temporal perturbations. For example, Yoshida et al. (2015a) inferred that the differential stress in the arc-backarc region must be rather low because earthquake focal mechanisms change with topographic variations of hundreds of meters. Yoshida et al. (2014, 2015b, 2016) also inferred very low differential stresses at local scales from observed sensitivity of the stress field to perturbations by medium-size earthquakes of magnitudes 6.4–7.2.

By slightly modifying the model of Figure 5, we further demonstrate the fragility of the state of stress in the offshore forearc. If the surface topography is oversimplified so that the surface slope of the outer wedge area is gentler (Figure 7a), the effect of the gravitational force is slightly reduced. In the example shown in Figure 7a, most of the offshore forearc is still under compression even though the megathrust μ_b' is only 0.025. Compared to models of correct geometry, the oversimplified geometry results in a larger average $\sigma_x - \sigma_z$ for the 50- to 100-km segment for any μ_b' value (Figure 7c). If the correct topography is used but the load by ocean water is ignored (Figure 7b), the effect is the opposite. Compared with models that include the water load, the forearc is more extensional for any μ_b' value (Figure 7c).

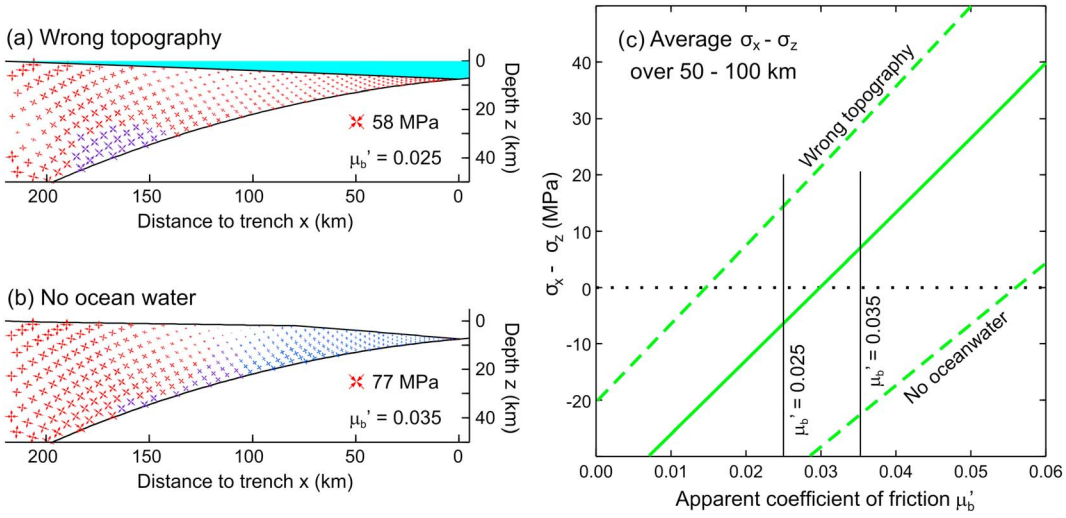

Figure 7. Testing models to illustrate the fragility of forearc state of stress. (a) Deviatoric stresses for a model with an oversimplified seafloor geometry. (b) Deviatoric stresses for a model neglecting the effect of ocean water load. In both (a) and (b), the meaning of the colors of the stress crosses is the same as in Figure 5. (c) Spatial averages of before-earthquake $\sigma_x - \sigma_z$ for the 50- to 100-km segment for the two types of models in (a) and (b) but with many different μ' values, in comparison with the models with correct seafloor geometry and ocean load (solid line).

4. Mechanical Stability of the Forearc

4.1. Wedge Mechanics

The elastic models used in section 3 are inadequate for the stability analysis because they cannot accommodate permanent deformation. For addressing the first-order mechanics, it is most convenient to apply the theory of dynamic Coulomb wedge (Wang & Hu, 2006). In this theory, the wedge-shaped offshore forearc is simplified as a material of elastic—perfectly plastic rheology (Figure 1c). Its similarity with the force balance model of Figure 1b is obvious. The classical Coulomb wedge theory considers only the plastic state, that is, a critically tapered wedge everywhere on the verge of Coulomb failure (Dahlen, 1984, 1990; Davis et al., 1983; Zhao et al., 1986). It emphasizes how the wedge geometry (surface slope angle α and basal dip β) is controlled by wedge strength and basal μ_b'. The dynamic theory considers both the critical and stable states (Wang & Hu, 2006). Given wedge geometry, it describes how the wedge can change from one critical state to another as controlled by μ_b' through an infinite number of stable states.

For this discussion, it suffices to use the analytical solutions for a uniform and cohesionless Coulomb wedge (Figure 1c) that were obtained by Dahlen (1984) and Wang and Hu (2006). The strength of such a wedge is represented by $\mu(1-\lambda)$, where μ is the coefficient of internal friction and λ is the pore fluid pressure ratio within the wedge. With parameters illustrated and defined in Figure 1c, λ is defined as

$$\lambda = \frac{P - \rho_w g D}{\sigma_z - \rho_w g D}, \tag{1}$$

where P is pore fluid pressure within the wedge. Because we use the rock mechanics convention of defining compressive stress as positive in this paper, the minus sign before σ_z seen in other Coulomb wedge papers is absent here. The basal shear stress can be expressed as a function of either the normal stress σ_n or the effective normal stress $\bar{\sigma}_n = \sigma_n(1-\lambda)$,

$$\tau = \mu_b' \sigma_n = \frac{\mu_b'}{1-\lambda} \bar{\sigma}_n. \tag{2}$$

In Dahlen (1984) and Wang and Hu (2006), the "effective coefficient of friction" referred to the parameter $\mu_b'/(1-\lambda)$. In Hu and Wang (2008) and this paper, it refers to μ_b', compatible with the common usage in Earth science as is obvious in Figure 1.

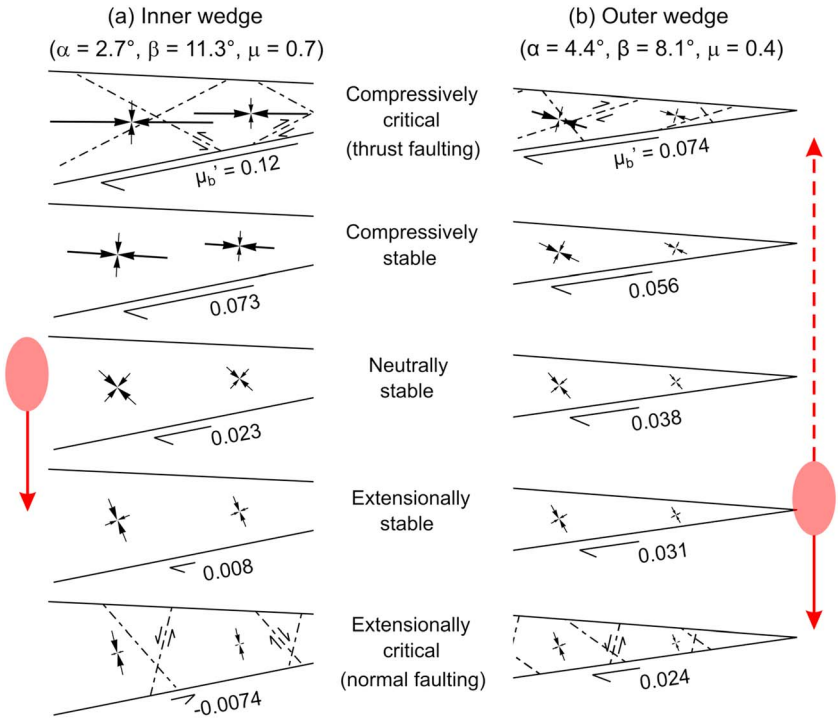

Figure 8. State of stress in an elastic-Coulomb plastic wedge. For critical states, dashed lines are plastic slip lines (potential failure planes) with sense of shear indicated. The neutral state is defined as the plunge of σ_1 being 45° from horizontal (not from the x axis shown in Figure 1c). The assumed wedge geometry is appropriate for the Japan Trench. Pore fluid pressure ratio in the wedge (equation (1)) is assumed to be 0.8. A red-filled ellipse marks the mechanical state before a great earthquake. (a) Inner wedge. Coseismic weakening of the megathrust (stress drop) during the Tohoku-Oki earthquake caused the wedge to change to a more extensional stable state (red arrow). (b) Outer wedge. Coseismic weakening of the basal fault in the Tohoku-Oki earthquake may have brought the wedge to extensional failure (solid red arrow). In some other great earthquakes, coseismic strengthening (negative stress drop) of the basal fault may bring the wedge toward compressive failure (dashed red arrow).

The strength of the basal fault (megathrust) can be expressed in a familiar form $\mu_b' = \mu_b(1-\lambda_b)$, where μ_b is the intrinsic friction coefficient of the fault and λ_b is the pore fluid pressure ratio within the fault zone. However, if the pore fluid pressure in the fault zone differs from that within the wedge, mathematical complications occur in the system shown in Figure 1c such that λ_b cannot be accurately defined using a form analogous to (1) unless $\alpha+\beta$ is much less than 10° (Wang et al., 2006). Therefore, it is simpler to focus only on μ_b', which is independent of the coordinate system, without explicitly invoking λ_b while keeping in mind that μ_b' reflects both the intrinsic fault friction and the effect of pore fluid pressure in the fault zone.

4.2. Inner Wedge Versus Outer Wedge

The inner wedge and outer wedge (Figure 1b) need to be considered separately. The inner wedge features a gentler surface slope and steeper basal dip (Figure 8a). We assume an internal friction coefficient of $\mu = 0.7$ for the inner wedge, similar to that of Byerlee's law (Byerlee, 1978), because it consists mostly of the rock framework of the crystalline upper-plate crust. The outer wedge features a steeper surface slope and gentler basal dip (Figure 8b). We assume $\mu = 0.4$ for the outer wedge because it contains much less consolidated and/or recently deformed material. We assume $\lambda = 0.8$ for both wedges. Note that here the important issue is the strength and geometrical contrast between the inner and outer wedges, not specific parameter values. For example, one could assume the same μ but contrasting λ values and reach similar conclusions. The most seaward portion of the outer wedge, typically within 10–15 km of the trench is the frontal prism (e.g., von Huene et al., 2009) that involves complex processes of sediment accretion, erosion, and recycling (e.g., Tsuji et al., 2011, 2013). Processes specific to the frontal prism are not included in our discussion.

A clarification needs to be made with regard to the model geometry of the inner wedge. For the inner wedge, the α or β values should not be derived locally from the surface slope and basal dip of the actual inner wedge

area (Figure 1b). The reason is that the inner wedge is connected to the outer wedge. If the actual local surface slope angle is used for α, the influence of the steeper slope of the outer wedge is neglected, and hence, the effect of gravity will be underestimated. If the local basal dip is used for β, the role of the gently dipping megathrust underlying the outer wedge is neglected, and hence, the effect of the basal shear will be underestimated. This point was overlooked in previous applications of the Coulomb wedge theory to the inner wedge such as Wang and Hu (2006). In this work, we choose to use the average values of α and β between the region of interest and the trench. It is still an approximation. With analytical solutions that do not handle spatially variable surface slope and basal dip, it is considered the best compromise.

Figure 8 shows how the inner and outer wedges may theoretically change from one critical state to another as controlled by the level of basal friction. If μ_b' were greater than that shown in the top panel of Figures 8a or 8b or lower than that in the bottom panel, the wedge would become unstable and would have to deform to attain new geometry. It is important to understand that the plunge of σ_1 in the wedge does not translate to wedge strength. There is a wide range of plunge for an elastic stable wedge, depending on the level of basal friction.

4.3. Stability of the Inner Wedge and Onshore-Nearshore Forearc

The strength of the inner wedge in Figure 8a is $\mu(1-\lambda) = 0.14$, much stronger than that of the megathrust $\mu_b' = 0.032$ (Figure 6). The inner wedge with this level of basal friction is stable, with a state of stress only slightly more compressive than neutral (Figure 8a). The stress state before the Tohoku-Oki earthquake is thus schematically marked by the red ellipse in Figure 8a. The megathrust stress drop in this or other great earthquake is a few MPa (Figure 2b), which brings the inner wedge toward a more extensional state (red arrow in Figure 8a). At 20-km depth, the megathrust shear stress is about 20 MPa if $\mu_b' = 0.032$. Even if the stress drop over a large area of the fault could be as large as 10 MPa, the corresponding weakening of the fault being 50%, the new μ_b' value of 0.016 still would define a stable inner wedge. No reasonable stress drop over a large enough fault area could bring the inner wedge to the critical state of extensional failure. In fact, the inner wedge would be in a theoretical state of extensional failure only if the basal shear could reverse direction to represent a normal fault (Figure 8a, bottom panel). The critical state of compressive failure is even more unlikely (Figure 8a, top panel). Therefore, the inner wedge is stable throughout the subduction earthquake cycles.

As shown in Figure 9a, the notion of a stable inner wedge in earthquake cycles is almost regardless of model parameters μ and λ. The strength of the continental crust is generally considered to be represented by Byerlee's law ($\mu \approx 0.7$) with hydrostatic pore fluid pressure ($\lambda \approx 0.4$; e.g., Townend & Zoback, 2000; Zoback & Townend, 2001). By assuming $\lambda \approx 0.8$, we have assumed a much weaker crust. Even so, a differential stress of a few tens of MPa is still far from critical. Figure 9a (dashed ellipse) shows that the wedge will be stronger and more stable if we assume a lower λ (although still higher than hydrostatic).

In summary, the observed stress change caused by the Tohoku-Oki earthquake does not indicate a weak inner wedge. Strength is even less relevant for the onshore-nearshore part of the forearc. The above reasoning is consistent with independent studies showing that differential stress in the Japan Trench forearc is only a few tens of MPa (Yoshida et al., 2014, 2015a, 2016).

4.4. Permanent Deformation and Crustal Stability

One seemingly intriguing issue is whether permanent deformation such as active faulting and earthquakes indicates a critical state of failure of the inner wedge (or in general the lithosphere). If there are temporal variations of the stress field, the wedge cannot always stay at a critical state. Then the question becomes whether it can reach a critical state sometimes, and when. Over the geological history of any region, there were certainly "moments" when the crust was critically stressed or even unstable, changing its structure and morphology in response to tectonic loading, to be further discussed in section 4.6. However, we have argued above (Figure 8a) that the inner wedge is too strong to enter a critical state in any phase of the subduction earthquake cycles.

If the inner wedge is far from a critical state of failure, why does it produce earthquakes that are manifestations of permanent brittle failure? The same paradoxical question applies to the nearshore and onshore forearc and farther inland. Regalla et al. (2010) reported geological evidence for active reverse faulting under

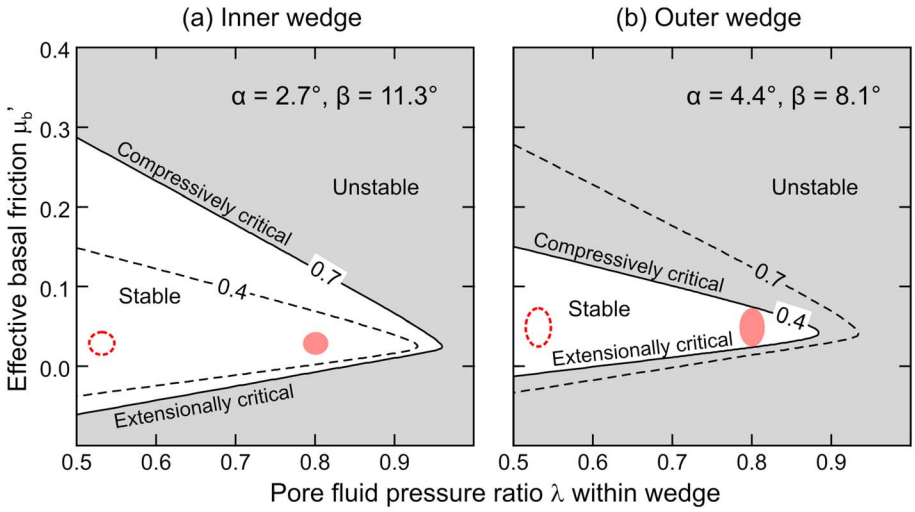

Figure 9. Mechanical states of the wedges shown in Figure 8 as controlled by basal friction μ_b' and pore fluid pressure ratio λ within the wedge. Red-filled ellipse illustrates the possible range of states in subduction earthquake cycles. Dashed ellipse illustrates the range for much lower λ (still higher than hydrostatic). (a) Inner wedge ($\mu = 0.7$), stable in earthquake cycles. Critical states for $\mu = 0.4$ are shown for comparison. (b) Outer wedge ($\mu = 0.4$) that may switch between the stable and two opposite critical states. Critical states for $\mu = 0.7$ are shown for comparison. Note that, because of the shallower depth of the basal fault beneath the outer wedge (and hence lower normal stress), a larger range of μ_b' in (b) than in (a) does not necessarily mean larger changes in fault shear stress.

margin-normal compression near the coast around latitude 37–37.5°. Does it not indicate a critical state? Our explanation is that these signs of permanent deformation reflect local failure in a strong, stable, but mechanically heterogeneous system, rather than pervasive failure of the system. By inference, such local failure must be geologically short-lived. While in some regions the crust appears to be critically stressed, at least at shallow depths (Townend & Zoback, 2000), the forearc of Japan Trench and probably of all subduction zones is generally not.

Throughout the Neogene, Northeast Japan went through a "tectonic inversion" from extension to shortening in the direction normal to the present Japan Trench margin, and many normal faults previously accommodating extension were reactivated as reverse faults (Sato, 1994), probably facilitated by extremely high pore fluid pressure (Sibson, 2009). This recent geological history leaves us with a badly scarred upper plate full of structural and stress heterogeneities. There is no surprise crustal earthquakes occur in various places in such a heterogeneous geological environment, and with good correlation with known geological structures (Yoshida et al., 2018), but the cumulative moments of these earthquakes are exceedingly small if compared with that accrued by the megathrust through seismic and aseismic slip.

Most of the early extension and later shortening occurred in the arc-backarc region (Kato, Sato, et al., 2006; Sato, 1994), consistent with its warm thermal state and hence thin lithosphere (Wada & Wang, 2009). The early extension also affected parts of the forearc (e.g., Toda & Tsutsumi, 2013). Some of the reactivated faults in the backarc still host small- to medium-size reverse-faulting earthquakes today (Kato, Sakai, et al., 2006), although it is possible that many of these structures were more active during the Pliocene when tectonic compression might be stronger than today. Geological evidence for ongoing margin-normal shortening of the forearc is extremely rare (Regalla et al., 2010). If the reverse faulting in the coastal forearc reported by Regalla et al. (2010) is still active, it must reflect local and possibly near-surface shortening under very low differential stress.

A good example of the crustal heterogeneity is provided by the small area of persistent shallow, normal-faulting earthquakes (Figure 2a) mentioned in the last paragraph of section 2.1. Surface rupture caused by an $M_w = 6.6$ Tohoku-Oki aftershock in this area indicates reactivation of old normal faults formed in the Neogene (Toda & Tsutsumi, 2013). However, one of the field sites of Regalla et al. (2010) showing active reverse faulting is only 10 km from this earthquake. As mentioned in section 2.1, crustal earthquakes deeper than 12 km in this area persistently show reverse faulting (Yoshida et al., 2015a). The very local, near-surface

extensional regime in this small area cannot possibly be geologically sustainable and does not represent the general mechanical state of the forearc. The geological conditions and processes responsible for the reversal of faulting mechanism over such short distances deserve further investigation.

4.5. On the Stability of the Outer Wedge

Based on structural and morphological contrasts, subduction zone outer wedge displays more characteristics of active deformation than does the inner wedge. Wang and Hu (2006) proposed that the outer wedge could achieve a compressively critical state during great earthquakes due to Coseismic Strengthening of the Shallow Megathrust (CSSM). If the red ellipse in Figure 8b represents the state of the outer wedge before a great earthquake, CSSM should cause the wedge to follow the path indicated by the red dashed arrow toward being more compressive during the earthquake. It is not immediately clear whether CSSM occurred during the 2011 Tohoku-Oki earthquake. Tsunamigenic large slip at the trench by no means excludes CSSM (Hu & Wang, 2008; Tsuda et al., 2017). Modeling of differential bathymetry in the trench area before and after the earthquake does suggest that the slip peaked at the trench at least along the central corridor through the rupture zone (Sun et al., 2017). Therefore, CSSM does not seem to have happened along this corridor. However, we do not know whether there was a general lack of CSSM everywhere along strike; both differential bathymetry (Sun et al., 2017) and seafloor structure observations (Tsuji et al., 2013) suggest variable behavior of the shallow megathrust along strike in the rupture area.

If the shallow megathrust actually underwent coseismic weakening in 2011 as opposed to CSSM, the outer wedge is expected to have followed the path of the solid red arrow in Figure 8b and possibly entered an extensionally critical state (with $\mu_b^{'} = 0.024$). Complete stress drop (i.e., $\mu_b^{'} = 0$ after the earthquake), although locally possible, is unlikely to have ever happened over a main fraction of the shallow megathrust in recent geological history; otherwise, the outer wedge would have become gravitationally unstable and collapsed under its own weight to attain a lower surface slope.

The shallow megathrust may not behave the same way in every great earthquake. There are different theories to explain the possible absence of CSSM in 2011. One theory is dynamic weakening (Di Toro et al., 2011; Kimura et al., 2012; Noda & Lapusta, 2013; Sun et al., 2017; Tsuda et al., 2017). In this theory, the shallow megathrust may normally exhibit rate strengthening at low slip rate, but if it is driven by extraordinarily large slip of the downdip seismogenic zone to acquire a high enough slip rate, it can dramatically weaken to participate in the seismic rupture. One may argue that dynamic weakening of the shallow megathrust requires a large enough size and rate of the seismic slip of its downdip neighbor (Cubas et al., 2015; Noda & Lapusta, 2013), such that CSSM may still occur in some earthquakes. Whether the outer wedge can be brought to the critical state of compressive failure depends on the degree of CSSM (Hu & Wang, 2008).

The strength of the outer wedge in Figure 8b is $\mu(1-\lambda) = 0.08$, weaker than the inner wedge. The shallow megathrust is less mature than its deeper counterpart and thus may exhibit a wider range of $\mu_b^{'}$ variation. If so, the outer wedge may exhibit a variety of behaviors in different earthquakes, sometimes stable, sometimes extensionally critical, and sometimes compressively critical. Its zone of stability in the $(\lambda, \mu_b^{'})$ space is illustrated in Figure 9b (red-shaded ellipse). If for a given time the outer wedge is locally stronger somewhere along the margin, such as due to a lower λ, it is more difficult for great earthquakes to bring it to a critical state (Figure 9b, dashed ellipse).

The mechanical response of the outer wedge to the Tohoku-Oki earthquake has also been studied by Cubas et al. (2013) and Fukao et al. (2014). They both preferred the same λ value of 0.8 as in this work. Cubas et al. (2013) obtained a preferred $\mu_b^{'}$ as high as 0.13 because they assumed (1) that the outer wedge had the "Byerlee strength" of $\mu = 0.8$ and (2) that the outer wedge was in a compressively critical state before the Tohoku-Oki earthquake. Based on our discussions above, both these assumptions are highly questionable. Also because of the assumption of the very strong wedge, their model outer wedge does not become extensionally critical until $\mu_b^{'}$ is as low as 0.003, which led to the inference of a complete stress drop. We have shown (Figures 8b and 9b) that a complete stress drop over a large fault area is not only unnecessary in theory but also unlikely to have ever happened in reality. Fukao et al. (2014) only considered an elastic wedge, which should in principle be similar to the near-trench part of our numerical model discussed in section 3 (Figure 4). Their reported preferred friction coefficient value of 0.2 is for the parameter $\mu_b^{'}/(1-\lambda)$ (see equation (2)), and the $\mu_b^{'}$ value they actually preferred is $0.2(1-\lambda) = 0.04$, not very far from our preferred value. Their

speculation of complete stress drop may be affected by the neglect of strength limit; that is, the wedge never becomes unstable for any decrease in μ_b'.

4.6. Dynamic Coulomb Wedge Beyond Earthquake Cycles

There is a need to expand the theory of Wang and Hu (2006) to beyond the earthquake-cycle time scale. Based on the study of frictional heating, Gao and Wang (2014) concluded that subduction zone megathrusts are generally weak ($\mu_b' \sim 0.03$) but some are stronger than others (up to $\mu_b' \sim 0.13$). It is reasonable to expect that an individual subduction zone may have experienced phases of weaker and stronger megathrust in its geological history, depending on changes in the properties, especially roughness, of the subducting seafloor. It is conceivable that when the megathrust is stronger, the outer wedge can be compressively critical or even unstable or that the critical state can be more readily achieved during great earthquakes with the help of CSSM. It is also conceivable that the opposite can happen when the megathrust is weaker. Larger-scale plate dynamics that causes a change in the rate of slab rollback or in fault dip can also cause instability of the wedge. The wedge geometry is shaped in these trying times. Once the geometry is established, the wedge can stay mechanically stable over a wide range of megathrust strengths (Figures 8b and 9b) and over a long time. In other words, today's geomorphology often only commemorates the most traumatic geological moments of the past.

5. Conclusions

1. In response to the average stress drop of a few MPa in the M = 9 Tohoku-Oki earthquake, Japan Trench forearc became more extensional. A review of reported earthquake focal mechanisms suggests a reversal of the state of stress offshore from compressive to extensional. Because of increasing errors farther offshore in the determination of earthquake depths, the stress reversal is better constrained in the inner wedge than in the outer wedge.
2. Forearc stresses before the Tohoku-Oki earthquake could not constrain the upper limit of the megathrust strength, but the stress reversal caused by the earthquake unequivocally indicates a very weak megathrust. In order to reproduce this reversal in a model that quantifies the effects of gravity and megathrust friction using the geometry and parameters described in sections 3.1 and 3.2, the effective coefficient of friction of the megathrust has to be $\mu_b' \approx 0.032$. A lower value would make the forearc too extensional before the earthquake, and a higher value would make it too compressive after the earthquake.
3. The very weak megathrust results in very low differential stresses in the upper plate, consistent with previously reported sensitivity of the state of stress to small perturbations. Applying the dynamic Coulomb wedge model, we demonstrate that the inner wedge, and by inference the nearshore-onshore forearc, is in a stable state throughout subduction earthquake cycles, far from failure.
4. The outer wedge is normally in a stable state but may reach an extensionally or compressively critical state during an earthquake, depending on the behavior of the shallow megathrust. Gravitational collapse of the outer wedge is prevented by a finite strength of the underlying shallow megathrust (e.g., $\mu_b' \geq 0.024$ in Figure 8b). Therefore, complete stress drop ($\mu_b' = 0$) is unlikely to have happened over the main part of the shallow megathrust except for limited local areas.
5. The presence of permanent deformation such as earthquakes and active faulting in the overall stable forearc can be explained by structural and stress heterogeneities. We propose that for the most part, the upper plate near a subduction zone is much below its yield stress and is an elastic body, but permanent deformation can locally occur in areas of low strength, high stress, and/or high fluid pressure.
6. The concept of dynamic Coulomb wedge (Wang & Hu, 2006) needs to be expanded to address time scales much beyond subduction earthquake cycles. The strength of the megathrust varies over geological time scales, affecting the stability of the outer wedge and its response to earthquake rupture.

Acknowledgments
All the data used in this paper have been previously published in referenced papers. We thank the associate editor and two anonymous reviewers for their comments and M. Sypus for assistance in producing Figure 2b. L. B. was supported by a Discovery Grant to K. W. from the Natural Sciences and Engineering Research Council of Canada. This is Geological Survey of Canada contribution 20180417.

References

Asano, Y., Saito, T., Ito, Y., Shiomi, K., Hirose, H., Matsumoto, T., et al. (2011). Spatial distribution and focal mechanisms of aftershocks of the 2011 off the Pacific coast of Tohoku Earthquake. *Earth, Planets and Space*, *63*(7), 669–673. https://doi.org/10.5047/eps.2011.06.016

Brodsky, E. E., Saffer, D., Fulton, P., Chester, F., Conin, M., Huffman, K., et al. (2017). The postearthquake stress state on the Tohoku megathrust as constrained by reanalysis of the JFAST breakout data. *Geophysical Research Letters*, *44*, 8294–8302. https://doi.org/10.1002/2017GL074027

Brown, L. (2015). Strength of Megathrust Faults: Insights from the 2011 M=9 Tohoku-oki Earthquake. M.Sc. Thesis, University of Victoria, 105 p.

Brown, L., Wang, K., & Sun, T. (2015). Static stress drop in the *M*w 9 Tohoku-Oki earthquake: Heterogeneous distribution and low average value. *Geophysical Research Letters*, *42*, 10,595–10,600. https://doi.org/10.1002/2015GL066361

Bürgmann, R. (2015). Weak subduction makes great quakes. *Science*, *349*(6253), 1162–1163. https://doi.org/10.1126/science.aac9625

Byerlee, J. D. (1978). Friction of rocks. *Pure and Applied Geophysics*, *116*(4-5), 615–626. https://doi.org/10.1007/BF00876528

Cubas, N., Avouac, J.-P., Leroy, Y. M., & Pons, A. (2013). Low friction along the high slip patch of the 2011 Mw 9.0 Tohoku-Oki earthquake required from the wedge structure and extensional splay faults. *Geophysical Research Letters*, *40*, 4231–4237. https://doi.org/10.1002/grl.50682

Cubas, N., Lapusta, N., Avouac, J.-P., & Perfettini, H. (2015). Numerical modeling of long-term earthquake sequences on the NE Japan megathrust: Comparison with observations and implications for fault friction. *Earth and Planetary Science Letters*, *419*, 187–198. https://doi.org/10.1016/j.epsl.2015.03.002

Dahlen, F. A. (1984). Noncohesive critical Coulomb wedge: An exact solution. *Journal of Geophysical Research*, *89*(B12), 10,125–10,133. https://doi.org/10.1029/JB089iB12p10125

Dahlen, F. A. (1990). Critical taper model of fold-and-thrust belts and accretionary wedges. *Annual Review of Earth and Planetary Sciences*, *18*(1), 55–99. https://doi.org/10.1146/annurev.ea.18.050190.000415

Davis, D. M., Suppe, J., & Dahlen, F. A. (1983). Mechanics of fold-and-thrust belts and accretionary wedges. *Journal of Geophysical Research*, *88*(B2), 1153–1172. https://doi.org/10.1029/JB088iB02p01153

Di Toro, G., Han, R., Hirose, T., De Paola, N., Nielsen, S., Mizoguchi, K., et al. (2011). Fault lubrication during earthquakes. *Nature*, *471*, 494–498.

Fukao, Y., Hori, T., & Kodaira, S. (2014). Stress and displacement fields in the outer wedge induced by megathrust earthquakes. *Journal of Geophysical Research: Solid Earth*, *119*, 4219–4232. https://doi.org/10.1002/2013JB010398

Gao, X., & Wang, K. (2014). Strength of stick-slip and creeping subduction megathrusts from heat flow observations. *Science*, *345*(6200), 1038–1041. https://doi.org/10.1126/science.1255487

Hardebeck, J. L. (2012). Coseismic and postseismic stress rotations due to great subduction zone earthquakes. *Geophysical Research Letters*, *39*, L21313. https://doi.org/10.1029/2012GL053438

Hardebeck, J. L. (2015). Stress orientations in subduction zones and the strength of subduction megathrust faults. *Science*, *349*(6253), 1213–1216. https://doi.org/10.1126/science.aac5625

Hasegawa, A., Yoshida, K., Asano, Y., Okada, T., Iinuma, T., & Ito, Y. (2012). Change in stress field after the 2011 great Tohoku-Oki earthquake. *Earth and Planetary Science Letters*, *355-356*, 231–243. https://doi.org/10.1016/j.epsl.2012.08.042

Hu, Y., & Wang, K. (2008). Coseismic strengthening of the shallow portion of the subduction fault and its effects on wedge taper. *Journal of Geophysical Research*, *113*, B12411. https://doi.org/10.1029/2008JB005724

Ide, S., Baltay, A., & Beroza, G. C. (2011). Shallow dynamic overshoot and energetic deep rupture in the 2011 *M*w 9.0 Tohoku-oki earthquake. *Science*, *332*(6036), 1426–1429. https://doi.org/10.1126/science.1207020

Iinuma, T., Hino, R., Kido, M., Inazu, D., Osada, Y., Ito, Y., et al. (2012). Coseismic slip distribution of the 2011 off the Pacific Coast of Tohoku Earthquake (M9.0) refined by means of seafloor geodetic data. *Journal of Geophysical Research*, *117*, B07409. https://doi.org/10.1029/2012JB009186

Imanishi, K., Ando, R., & Kuwahara, Y. (2012). Unusual shallow normal-faulting earthquake sequence in compressional northeast Japan activated after the 2011 off the Pacific coast of Tohoku earthquake. *Geophysical Research Letters*, *39*, L09306. https://doi.org/10.1029/2012GL051491

Ito, Y., Sekiguchi, S., Okada, T., Honda, R., Obara, K., & Hori, S. (2006). Performance of regional distance centroid moment tensor inversion applied to the 2004 mid-Niigata prefecture earthquake, Japan. *Geophysical Journal International*, *167*(3), 1317–1331. https://doi.org/10.1111/j.1365-246X.2006.03109.x

Kagan, Y. Y. (1991). 3-D rotation of double-couple earthquake sources. *Geophysical Journal International*, *106*(3), 709–716. https://doi.org/10.1111/j.1365-246X.1991.tb06343.x

Kato, A., Sakai, S., Hirata, N., Kurashimo, E., Iidaka, T., Iwasaki, T., & Kanazawa, T. (2006). Imaging the seismic structure and stress field in the source region of the 2004 mid-Niigata prefecture earthquake: Structural zones of weakness and seismogenic stress concentration by ductile flow. *Journal of Geophysical Research*, *111*, B08308. https://doi.org/10.1029/2005JB004016

Kato, A., Sakai, S., & Obara, K. (2011). A normal-faulting seismic sequence triggered by the 2011 off the Pacific coast of Tohoku Earthquake: Wholesale stress regime changes in the upper plate. *Earth, Planets and Space*, *63*(7), 43.

Kato, N., Sato, H., & Umino, N. (2006). Fault reactivation and active tectonics on the fore-arc side of the back-arc rift system, NE Japan. *Journal of Structural Geology*, *28*(11), 2011–2022. https://doi.org/10.1016/j.jsg.2006.08.004

Kimura, G., Hina, S., Hamada, Y., Kameda, J., Tsuji, T., Kinoshita, M., & Yamaguchi, A. (2012). Runaway slip to the trench due to rupture of a highly pressurized megathrust beneath the middle trench slope: The tsunamigenesis of the 2011 Tohoku earthquake off the east coast of northern Japan. *Earth and Planetary Science Letters*, *339–340*, 32–45.

Lamb, S. (2006). Shear stresses on megathrusts: Implications for mountain building behind subduction zones. *Journal of Geophysical Research*, *111*, B07401. https://doi.org/10.1029/2005JB003916

Lin, W., Conin, M., Moore, J. C., Chester, F. M., Nakamura, Y., Mori, J. J., et al. (2013). Stress state in the largest displacement area of the 2011 Tohoku-Oki earthquake. *Science*, *339*(6120), 687–690. https://doi.org/10.1126/science.1229379

Luo, G., & Liu, M. (2009). Why short-term crustal shortening leads to mountain building in the Andes, but not in Cascadia? *Geophysical Research Letters*, *36*, L08301. https://doi.org/10.1029/2009GL037347

Magee, M. E., & Zoback, M. D. (1993). Evidence for a weak interplate thrust fault along the northern Japan subduction zone and implications for the mechanics of thrust faulting and fluid expulsion. *Geology*, *21*(9), 809–812. https://doi.org/10.1130/0091-7613(1993)021<0809:EFAWIT>2.3.CO;2

McKenzie, D., & Jackson, J. (2012). Tsunami earthquake generation by the release of gravitational potential energy. *Earth and Planetary Science Letters*, 345–348, 1–8.

Nakamura, W., Uchida, N., & Matsuzawa, T. (2016). Spatial distribution of the faulting types of small earthquakes around the 2011 Tohoku-Oki earthquake: A comprehensive search using template events. *Journal of Geophysical Research: Solid Earth*, *121*, 2591–2607. https://doi.org/10.1002/2015JB012584

Noda, H., & Lapusta, N. (2013). Stable creeping fault segments can become destructive as a result of dynamic weakening. *Nature*, *493*(7433), 518–521. https://doi.org/10.1038/nature11703

Obana, K., Kodaira, S., Shinohara, M., Hino, R., Uehira, K., Shiobara, H., et al. (2013). Aftershocks near the updip end of the 2011 Tohoku-Oki earthquake. *Earth and Planetary Science Letters*, *382*, 111–116. https://doi.org/10.1016/j.epsl.2013.09.007

Okada, T., Keisuke, Y., Sadato, U., Junichi, N., Naoki, U., Toru, M., et al., & Group for the aftershock observations of the 2011 off the Pacific coast of Tohoku Earthquake (2011). Shallow inland earthquakes in NE Japan possibly triggered by the 2011 off the Pacific coast of Tohoku earthquake. *Earth, Planets and Space*, *63*(7), 749–754. https://doi.org/10.5047/eps.2011.06.027

Regalla, C., Fisher, D., & Kirby, E. (2010). Timing and magnitude of shortening within the inner fore arc of the Japan Trench. *Journal of Geophysical Research*, *115*, B03411. https://doi.org/10.1029/2009JB006603

Satake, K., Fujii, Y., Harada, T., & Namegaya, Y. (2013). Time and space distribution of coseismic slip of the 2011 Tohoku earthquake inferred from tsunami waveform data. *Bulletin of the Seismological Society of America*, *103*(2B), 1473–1492. https://doi.org/10.1785/0120120122

Sato, H. (1994). The relationship between late Cenozoic tectonic events and stress field and basin development in northeast Japan. *Journal of Geophysical Research*, *99*(B11), 22,261–22,274. https://doi.org/10.1029/94JB00854

Seno, T. (2009). Determination of the pore fluid pressure ratio at seismogenic megathrusts in subduction zones: Implications for strength of asperities and Andean-type mountain building. *Journal of Geophysical Research*, *114*, B05405. https://doi.org/10.1029/2008JB005889

Shao, G., Chen, J., & Archuleta, R. (2012). Quality of earthquake source models constrained by teleseismic waves: Using the 2011 M9 Tohoku-Oki earthquake as an example, Poster 93 presented at Incorporated Research Institutions for Seismology Workshop, Boise, Idaho, 13–15 June.

Sibson, R. H. (2009). Rupturing in overpressured crust during compressional inversion—The case from NE Honshu, Japan. *Tectonophysics*, *473*(3-4), 404–416. https://doi.org/10.1016/j.tecto.2009.03.016

Sobolev, S. V., & Babeyko, A. Y. (2005). What drives orogeny in the Andes? *Geology*, *33*(8), 617–620. https://doi.org/10.1130/G21557.1

Sun, T., Wang, K., Fujiwara, T., Kodaira, S., & He, J. (2017). Large fault slip peaking at trench in the 2011 Tohoku-Oki earthquake. *Nature Communications*, *8*(1). https://doi.org/10.1038/ncomms14044

Toda, S., & Tsutsumi, H. (2013). Simultaneous reactivation of two, subparallel, inland normal faults during the M_w 6.6 11 April 2011 Iwaki earthquake triggered by the M_w 9.0 Tohoku-oki, Japan, Earthquake. *Bulletin of the Seismological Society of America*, *103*(2B), 1584–1602. https://doi.org/10.1785/0120120281

Townend, J., & Zoback, M. D. (2000). How faulting keeps the crust strong. *Geology*, *28*(5), 399–402. https://doi.org/10.1130/0091-7613(2000)28<399:HFKTCS>2.0.CO;2

Tsuda, K., Iwase, S., Uratani, H., Ogawa, S., Watanabe, T., Miyakoshi, J., & Ampuero, J. P. (2017). Dynamic rupture simulations based on the characterized source model of the Tohoku earthquake. *Pure and Applied Geophysics*, *174*(9), 3357–3368. https://doi.org/10.1007/s00024-016-1446-1

Tsuji, T., Kawamura, K., Kanamatsu, T., Kasaya, T., Fujikura, K., Ito, Y., et al. (2011). Potential tsunamigenic faults of the 2011 off the Pacific coast of Tohoku Earthquake. *Earth, Planets and Space*, *63*(7), 831–834. https://doi.org/10.5047/eps.2011.05.028

Tsuji, T., Kawamura, K., Kanamatsu, T., Kasaya, T., Fujikura, K., Ito, Y., et al. (2013). Extension of continental crust by anelastic deformation during the 2011 Tohoku-oki earthquake: The role of extensional faulting in the generation of a great tsunami. *Earth and Planetary Science Letters*, *364*, 44–58. https://doi.org/10.1016/j.epsl.2012.12.038

von Huene, R., Ranero, C. R., & Scholl, D. W. (2009). Convergent margin structure in high-quality geophysical images and current kinematic and dynamic models. In S. Lallemand, & F. Funiciello (Eds.), *Subduction Zone Geodynamics*, *Frontiers in Earth Sciences* (pp. 137–157). Berlin, Heidelberg: Springer. https://doi.org/10.1007/978-3-540-87974-9_8

Wada, I., & Wang, K. (2005). Effects of plate coupling and margin topography on forearc stresses. *Eos Trans. AGU, 86*(52), Fall Meet. Suppl., Abstract T33B-0542.

Wada, I., & Wang, K. (2009). Common depth of decoupling between the subducting slab and mantle wedge: Reconciling diversity and uniformity of subduction zones. *Geochemistry, Geophysics, Geosystems*, *10*, Q10009. https://doi.org/10.1029/2009GC002570

Wang, K., & He, J. (1999). Mechanics of low-stress forearcs: Nankai and Cascadia. *Journal of Geophysical Research*, *104*(B7), 15,191–15,205. https://doi.org/10.1029/1999JB900103

Wang, K., He, J., & Hu, Y. (2006). A note on pore fluid pressure ratios in the Coulomb wedge theory. *Geophysical Research Letters*, *33*, L19310. https://doi.org/10.1029/2006GL027233

Wang, K., & Hu, Y. (2006). Accretionary prism in subduction earthquake cycles: The theory of dynamic Coulomb wedge. *Journal of Geophysical Research*, *111*, B06410. https://doi.org/10.1029/2005JB004094

Wang, K., Sun, T., Brown, L., Hino, R., Tomita, F., Kido, M., et al. (2018). Learning from crustal deformation associated with the M = 9 2011 Tohoku-Oki earthquake. *Geosphere*, *14*(2), 552–571. https://doi.org/10.1130/GES01531.1

Wang, K., & Suyehiro, K. (1999). How does plate coupling affect crustal stresses in northeast and southwest Japan? *Geophysical Research Letters*, *26*(15), 2307–2310. https://doi.org/10.1029/1999GL900528

Yoshida, K. (2014). Study on the stress field in the crust in NE Japan obtained by focal mechanism, Ph.D. Thesis, Tohoku University, 144 p (in Japanese).

Yoshida, K., Hasegawa, A., & Okada, T. (2015a). Spatial variation of stress orientations in NE Japan revealed by dense seismic observations. *Tectonophysics*, *647-648*, 63–72. https://doi.org/10.1016/j.tecto.2015.02.013

Yoshida, K., Hasegawa, A., & Okada, T. (2015b). Spatially heterogeneous stress field in the source area of the 2011 Mw 6.6 Fukushima-Hamadori earthquake, NE Japan, probably caused by static stress change. *Geophysical Journal International*, *201*, 1060–1069.

Yoshida, K., Hasegawa, A., & Okada, T. (2016). Heterogeneous stress field in the source area of the 2003 M6. 4 Northern Miyagi Prefecture, NE Japan, earthquake. *Geophysical Journal International*, *206*(1), 408–419. https://doi.org/10.1093/gji/ggw160

Yoshida, K., Hasegawa, A., Okada, T., & Iinuma, T. (2014). Changes in the stress field after the 2008 M7.2 Iwate-Miyagi Nairiku earthquake in northeastern Japan. *Journal of Geophysical Research: Solid Earth*, *119*, 9016–9030. https://doi.org/10.1002/2014JB011291

Yoshida, K., Hasegawa, A., Okada, T., Iinuma, T., Ito, Y., & Asano, Y. (2012). Stress before and after the 2011 Great Tohoku-Oki earthquake and induced earthquakes in inland areas of eastern Japan. *Geophysical Research Letters*, *39*, L03302. https://doi.org/10.1029/2011GL049729

Yoshida, K., Hasegawa, A., Yoshida, T., & Matsuzawa, T. (2018). Heterogeneities in stress and strength in Tohoku and its relationship with earthquake sequences triggered by the 2011 M9 Tohoku-oki Earthquake. *Pure and Applied Geophysics*, *176*(3), 1335–1355. https://doi.org/10.1007/s00024-018-2073-9

Zhao, W. L., Davis, D. M., Dahlen, F. A., & Suppe, J. (1986). Origin of convex accretionary wedges: Evidence from Barbados. *Journal of Geophysical Research*, *91*(B10), 10,246–10,258. https://doi.org/10.1029/JB091iB10p10246

Zoback, M. D., & Townend, J. (2001). Implications of hydrostatic pore pressures and high crustal strength for the deformation of intraplate lithosphere. *Tectonophysics*, *336*(1-4), 19–30. https://doi.org/10.1016/S0040-1951(01)00091-9